Published OnlineFirst May 8, 2012; DOI: 10.1158/0008-5472.CAN-11-3931

Identification of Anaplastic Lymphoma Kinase as a Potential Therapeutic Target in Ovarian Cancer

Hong Ren[1], Zhi-Ping Tan[2,3], Xin Zhu[4], Katherine Crosby[1], Herbert Haack[1], Jian-Min Ren[1], Sean Beausoleil[1], Albrecht Moritz[1], Gregory Innocenti[1], John Rush[1], Yi Zhang[4], Xin-Min Zhou[3], Ting-Lei Gu[1], Yi-Feng Yang[2,3], and Michael J. Comb[1]

Abstract

Ovarian cancer is the leading cause of death from gynecologic cancer. Improvement in the clinical outcome of patients is likely to be achieved by the identification of molecular events that underlie the oncogenesis of ovarian cancer. Here we show that the anaplastic lymphoma kinase (ALK) is aberrantly activated in ovarian cancer. Using an unbiased and global phosphoproteomic approach, we profiled 69 Chinese primary ovarian tumor tissues and found ALK to be aberrantly expressed and phosphorylated in 4 tumors. Genetic characterization of these ALK-positive tumors indicated that full-length ALK expression in two serous carcinoma patients is consistent with *ALK* gene copy number gain, whereas a stromal sarcoma patient carries a novel transmembrane *ALK* fusion gene: *FN1-ALK*. Biochemical and functional analysis showed that both full-length ALK and FN1-ALK are oncogenic, and tumors expressing ALK or FN1-ALK are sensitive to ALK kinase inhibitors. Furthermore, immunohistochemical analysis of ovarian tumor tissue microarray detected aberrant ALK expression in 2% to 4% serous carcinoma patients. Our findings provide new insights into the pathogenesis of ovarian cancer and identify ALK as a potential therapeutic target in a subset of serous ovarian carcinoma and stromal sarcoma patients. *Cancer Res; 72(13); 3312–23. ©2012 AACR.*

Introduction

Ovarian cancer is the fifth leading cause of death from cancer in women, following lung, breast, colon, and pancreatic cancers. In 2011, a total of 21,990 new cases and 15,460 deaths of ovarian cancer were projected in the United States (The SEER Program of NCI). More than 90% ovarian cancer cases are epithelial cancer, which represents a series of molecularly and etiologically distinct diseases (1). Epithelial ovarian cancer can be grouped into 2 types. Type I tumors are genetically stable and confined to the ovary at presentation. It includes low-grade serous, low-grade endometrioid, clear cell, mucinous, and Brenner carcinomas, 90% of which are curable. In contrast, type II tumors, including high-grade serous carcinoma, undifferentiated carcinoma, and malignant mixed mesodermal tumors are highly aggressive and usually present in advanced stages (2). Most type II tumors bear *TP53* mutations and share no genetic alterations found in type I tumors (2, 3). High-grade serous carcinoma stands out from other subtypes because it accounts for 60% to 80% of ovarian cancer cases and most deaths from ovarian cancer. Recent studies have shown that high-grade serous carcinoma may arise from fallopian tube epithelium other than ovary itself (1, 4, 5). Because of the subtle nature of symptoms and inadequate screening tools, most serous ovarian carcinoma patients present at advanced stages with poor prognosis (2, 6). Although initial response rates to standard surgery and chemotherapy are high, the disease recurs in the majority of patients and eventually becomes chemoresistant (7). The fact that the overall survival rate for women with ovarian cancer has not changed over the last 30 years demands new therapeutic approaches. With advances in understanding the genetics and molecular biology of ovarian cancer, targeted therapy will likely have a significant impact on overcoming chemoresistant disease and improvement of patient outcome (1, 6, 8).

Oncogenic receptor tyrosine kinases (RTK) have been implicated in many types of solid tumors, including ovarian cancer. A recent report by Sheng and colleagues showed that an NRG1-Her3 autocrine loop could promote ovarian cancer cell proliferation (9). Overexpression of other RTKs, such as

Authors' Affiliations: [1]Cell Signaling Technology, Inc., Danvers, Massachusetts; [2]Clinical Center for Gene Diagnosis and Therapy of the State Key Laboratory of Medical Genetics, [3]Department of Cardiothoracic Surgery, The Second Xiangya Hospital, and [4]Department of Gynecology and Obstetrics, Xiangya Hospital, Central South University, Changsha, Hunan, China

Note: Supplementary data for this article are available at Cancer Research Online (http://cancerres.aacrjournals.org/).

H. Ren and Z.-P. Tan contributed equally to this work.

Corresponding Authors: Michael J. Comb, Cell Signaling Technology, Inc., Danvers, MA 01923. Phone: 978-876-2315; Fax: 978-867-2400; E-mail: mcomb@cellsignal.com; Ting-Lei Gu, E-mail: tgu@cellsignal.com; and Yi-Feng Yang, Clinical Center for Gene Diagnosis and Therapy of the State Key Laboratory of Medical Genetics, and Department of Cardiothoracic Surgery, The Second Xiangya Hospital, Central South University, Changsha, Hunan 410011, China. E-mail: yyf627@163.com

doi: 10.1158/0008-5472.CAN-11-3931

Published OnlineFirst May 8, 2012; DOI: 10.1158/0008-5472.CAN-11-3931

EGF receptor (EGFR), Her2, Her3, platelet-derived growth factor receptor, and EphA2, was reported in ovarian cancer (10–13). However, it remains to be determined whether these RTKs play any roles in tumor initiation and progression in ovarian cancer.

In this article, we used an immunoaffinity profiling approach (14–16) to identify activated tyrosine kinases in 69 primary ovarian tumors. Our results indicate that many RTKs are aberrantly phosphorylated in tumors. Most interestingly, phosphorylation of anaplastic lymphoma kinase (ALK) is identified in 3 high-grade serous carcinoma patients and one stromal tumor patient. When activated by mutations or translocations, ALK can drive oncogenesis in non-Hodgkin lymphoma (17), neuroblastoma (18–21), non–small cell lung cancer (NSCLC) (15, 22), inflammatory myofibroblastic tumor (23), and renal cell carcinoma (24, 25). Our biochemical and functional analysis suggests that, as it does in other malignancies, ALK is likely driving a subset of ovarian cancers and could be a new drug target in this devastating disease.

Materials and Methods

Patients, tissue specimens, and pathologic data

Ovarian tissues were collected randomly from 69 ovarian tumor patients and 19 patients with benign gynecologic conditions who needed oophorectomy in the Xiangya Hospital (Changsha, Hunan, China) from February 2009 to February 2010 with written consent from the patients (Institutional Review Board approval). Tissue specimens were taken intraoperatively and were either formalin-fixed and paraffin-embedded (FFPE) or snap frozen in liquid nitrogen. Histologic typing and grading were carried out according to International Federation of Gynecology and Obstetrics (FIGO) guidelines. General pathologic information of the 69 ovarian tumor patients is listed in Supplementary Table S1. FFPE ovarian tumor tissue microarray (TMA) slides were purchased from Folio Biosciences and Biochain Institute, Inc.

Cell lines and antibodies

Ovarian cancer cell lines Ovsaho, Ovmana, and Ovmiu are purchased from Japanese Collection of Research Bioresources/Health Science Research Resources Bank. Antibodies against ALK (D5F3 XP), phospho-ALK (Y1278/1282/1283), SHC, phospho-SHC (Y234/240), Erk, phospho-Erk (T202/Y204), Stat3, phospho-Stat3(Y705), phospho-AKT (S473), phospho-S6 (S235/236), CDC2 (CDK1), phospho-CDC2 (Y15), and β-actin are from Cell Signaling Technology, Inc.

Phosphotyrosine peptide profiling by PhosphoScan

An average of 15 milligrams of peptides were prepared from 0.2 to 0.5 grams of resected frozen ovarian tissues by homogenization, trypsin digestion, and Sep-pak C18 column purification as described previously (14–16). Peptides containing phosphotyrosine were isolated by immunoprecipitation with a monoclonal antibody (mAb) against phosphotyrosine (pY100), concentrated on reverse-phase micro tips and analyzed by liquid chromatography tandem mass spectrometry (LC/MS–MS). Briefly, samples were collected with an LTQ-Orbitrap mass spectrometer, using a top-ten method, a dynamic exclusion repeat count of 1, and a repeat duration of 30 seconds. MS and MS/MS spectra were collected in the Orbitrap and LTQ component of the mass spectrometer, respectively. SORCERER-SEQUEST (TM, v4.0.3 (c) 2008; Sage-N Research, Inc.) searches were done against the NCBI human RefPept database downloaded on January 6, 2009 (containing 37,742 proteins) or March 1, 2010 (containing 36,500 proteins), allowing for serine, threonine, and tyrosine phosphorylation (STY+80) and methionine oxidation (M+16) as differential modifications. The PeptideProphet probability threshold was chosen to give a false positive rate of 5% for the peptide identification (26).

Clustering and ranking analysis

To assess potentially aberrant tyrosine phosphorylation of RTK in tumor tissues, spectral counts per RTK were summed and normalized to the amount of peptide subjected to phosphotyrosine immunoprecipitation (15 mg), elevated spectral count in each tumor sample was calculated by subtracting average spectral count in 19 normal ovarian tissues. Elevated phosphotyrosine spectral counts of RTKs, representing elevated tyrosine phosphorylation, observed in 60 tumor samples were used as basis for hierarchical Clustering using the Pearson correlation distance metric and average linkage (MultiExperiment Viewer version 4.4). RTKs with elevated phosphorylation in tumors are ranked based on the average value of elevated spectral count in corresponding tumors.

Western blot

Frozen ovarian tumor tissue were minced in liquid nitrogen and resuspended in 1× cell lysis buffer. Tissue or cell suspension was then sonicated and cleared by centrifugation. Immunoblot analysis was carried out according to the manufacturer's standard protocol (www.cellsignal.com).

5′-Rapid amplification of cDNA ends

RNeasy Mini Kit (Qiagen) was used to extract RNA from human tumor samples. Rapid amplification of cDNA ends (RACE) was done with the use of 5′-RACE system (Invitrogen) with primer 5′-GCAGTAGTTGGGGTTGTAGTC for cDNA synthesis and 5′-GCGGAGCTTGCTCAGCTTGT and 5′-TGCAGCTCCTGGTGCTTCC for a nested PCR reaction, followed by cloning and sequencing the PCR products.

Reverse transcription PCR

RNA was extracted from ovarian tumor tissue or cell lines using RNeasy Mini Kit (Qiagen). For reverse transcription PCR (RT-PCR), first-strand cDNA was synthesized from 2.5 mg of total RNA using SuperScript III first-strand synthesis system (Invitrogen) with oligo $(dT)_{20}$. Primer pairs used to amplify wild-type ALK and FN1-ALK transcripts were 5′-GAGGATATATAGGCGGCAAT, 5′-TGCAGCTCCTGGTGCTTCC, and 5′-TAAGCTGGGTGTACGACCAA, 5′TGCAGCTCCTGGTGCTTCC, respectively. Transcripts from the control gene glyceraldehyde-3-phosphate dehydrogenase (*GAPDH*) were amplified using primer pairs 5′-GATTCCACCCATGGCAAATTCC and 5′-GATTCCACCCATGGCAAATTCC.

Published OnlineFirst May 8, 2012; DOI: 10.1158/0008-5472.CAN-11-3931

Quantitative PCR assay

DNeasy Blood & Tissue Kit (Qiagen) was used to extract genomic DNA from frozen ovarian tumor samples. Quantitative PCR (qPCR) was done using iQ SYBR Green Supermix (Bio-Rad). Each qPCR reaction contains 10 μL of SYBR Green Master Mix, 1 μL of 10 nmol/L forward primer, 1 μL of 10 nmol/L reverse primer, 6 μL of nuclease free water, and 2 μL of genomic DNA at 10 ng/mL. qPCR reaction was carried out with the following parameters: 95°C for 10 minutes followed by 40 cycles of 95°C for 15 seconds and 65°C for 15 seconds. A dissociation run from 55°C to 95°C was added to the end of qPCR reaction for melting curve analysis. Nonspecific amplification was not detected with the primers used in the study. PCR reactions were set up in duplicates for each sample tested. Data were exported from CFX96 Real-Time PCR Detection System and analyzed using Microsoft Excel. We used an Ultra Conservative Element (UCE) located on human Chromosome 7 (Chr7: 1,234,865–1,235,026) that has been identified to have a copy number of 2 as reference DNA segment and calculated the ΔC_t by subtracting the C_t value of the UCE reactions from that of the ALK reactions in each sample. This normalizes the variation in the amount of templates between samples. We then used ΔC_t values from each individual to calculate relative copy number against calibrator DNA isolated from NA10851 (Coriell Cell Repository). Calculations were carried out to normalize a copy number of 2 to a value of 1 in the bar graph. SDs were based on normalized C_t values of duplicates. The sequences of the primers that are used to amplify *ALK* gene are 5′-ACAAGGTCCACGGATCCAGAAACA and 5′-AGTCTCCCAGTTGCAACGTTAGGT.

Constructs and the establishment of 3T3 cell lines stably expressing FN1-ALK and wild-type ALK

The coding sequences of wild-type ALK and FN1-ALK were cloned from primary tumor samples OC26 and OC19, respectively, into retroviral vector MSCV-Neo. The expression plasmids were transfected into 293T cells by FuGene 6 (Roche Diagnositcs), and retrovirus was harvested 48 hours later. NIH3T3 cells were infected with MSCV-neo/ALK or MSCV-neo/FN1ALK and selected in G418-containing media for 7 days. The cells were then cultured in soft agar or injected subcutaneously into nude mice.

Tumor grafts and *in vivo* drug sensitivity studies

A total of 1.5×10^6 to 2×10^6 transduced 3T3 cells expressing Src, FN1-ALK, or ALK were resuspended in Matrigel (BD Biosciences) and injected subcutaneously into the upper or lower right flank of 6 to 8 weeks old female NCR NU-F mice purchased from Taconic. Mice were randomized to 3 treatment groups ($n = 6$ per group) once the tumors became palpable (~50 mm^3) and gavaged orally with vehicle (10% 1-methy-2-pyrrolidinone/90% PEG-300) alone, 100 mg/kg/d crizotinib or 10 mg/kg/d TAE684 (NVP-TAE684) for 7 to 11 days. Crizotinib and TAE684 were purchased from ChemieTek. Tumors were measured every other day using calipers, and tumor volume was calculated as $0.52 \times \text{width}^2 \times \text{length}$. Mice were monitored daily for general conditions. The experiment was terminated when the mean size of the treated or control mice reached 1,500 mm^3. Animal protocol is in accordance with Cell Signaling Technology Animal Care and Use Committee with approval ID 650.

Table 1. Characteristics of ovarian cancer patients

	All patients ($n = 69$)
Characteristics	**No. (%)**
I. Age at surgery, y	
Median 47	
Range 14–65	
14–40	16 (23.2)
41–55	40 (58.0)
>55	13 (18.8)
II. Histologic type	
Adenocarcinoma	52 (75.8)
Serous	43
Endometrioid	3
Mucinous	5
Clear cell	1
Stromal tumor	6 (8.7)
Granulosa–Theca cell tumor	4
Sarcoma	2
Others	11 (15.9)
Secondary tumor	5
Malignant Brenner tumor	1
Teratoma	3
Squamous carcinoma	2

Results

Identification of ALK phosphorylation in ovarian tumor tissues by LC/MS–MS mass spectrometry

To identify oncogenic kinases in ovarian tumors, we carried out immunoaffinity profiling of tyrosine phosphorylation in 69 tumor and 19 normal tissues with PhosphoScan (14). The characteristics of the 69 ovarian cancer patients are summarized in Table 1. Most of the 43 serous type tissues were high-grade serous carcinoma characterized by cancerous spreading in the pelvic area. LC/MS–MS identified 2,484 tyrosine phosphorylation sites in 1,349 proteins, with global false discovery rate to be less than 5% using peptide prophet (26). These data are available at PhosphoSitePlus (www.phosphosite.org). Spectral counts for all phosphotyrosine sites identified in tyrosine kinases across the 88 ovarian tissues are listed in Supplementary Table S2.

Previous studies have shown that elevated tyrosine phosphorylation of RTKs may represent aberrant kinase activity in tumor tissues, which could drive oncogenesis (15). Using RTK tyrosine phosphorylation in 19 normal ovarian tissues as basal phosphorylation level, we assessed potentially aberrant tyrosine phosphorylation of RTKs in tumor tissues. As shown in Fig. 1A, we observed elevated tyrosine phosphorylation in many RTKs across the 60 tumor tissues, including

Published OnlineFirst May 8, 2012; DOI: 10.1158/0008-5472.CAN-11-3931

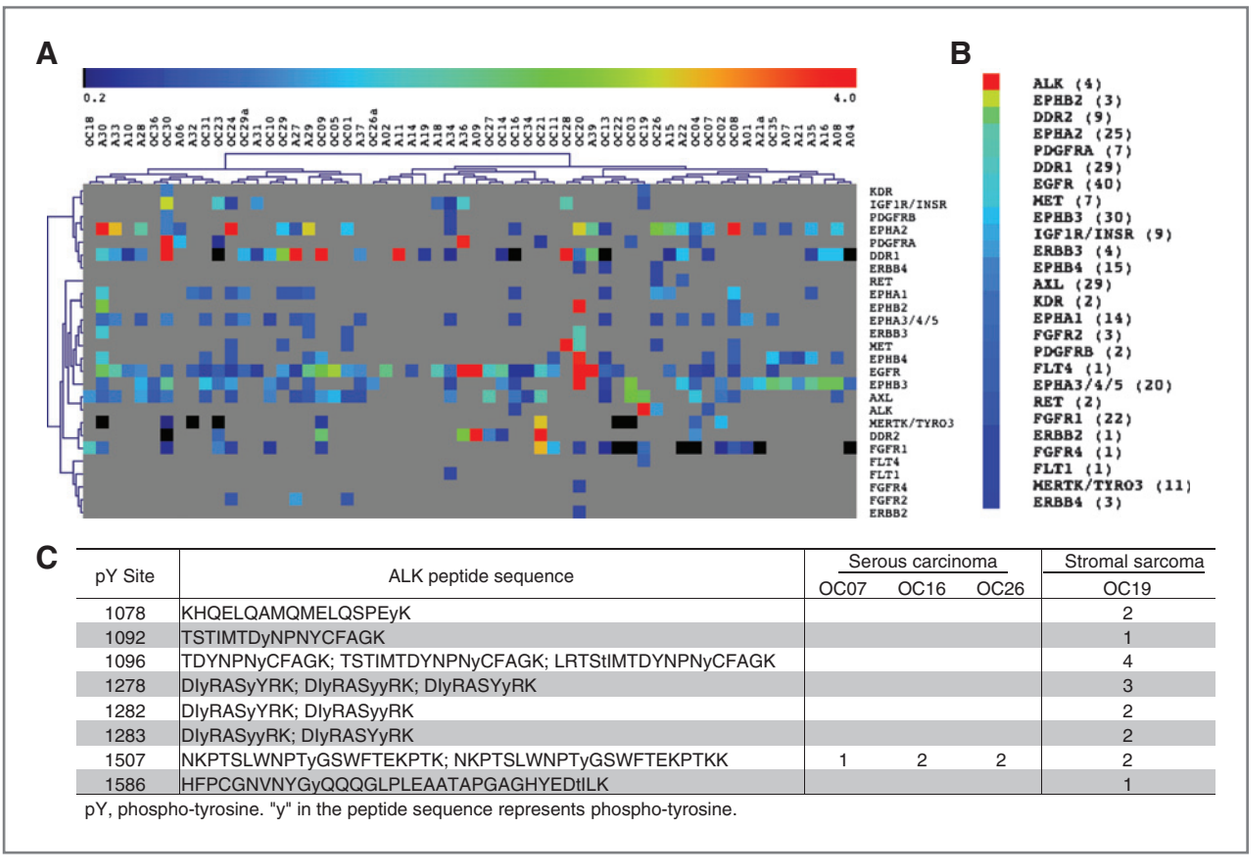

C

pY Site	ALK peptide sequence	Serous carcinoma			Stromal sarcoma
		OC07	OC16	OC26	OC19
1078	KHQELQAMQMELQSPEyK				2
1092	TSTIMTDyNPNYCFAGK				1
1096	TDYNPNyCFAGK; TSTIMTDYNPNyCFAGK; LRTStIMTDYNPNyCFAGK				4
1278	DIyRASyYRK; DIyRASyyRK; DIyRASYyRK				3
1282	DIyRASyYRK; DIyRASyyRK				2
1283	DIyRASyyRK; DIyRASYyRK				2
1507	NKPTSLWNPTyGSWFTEKPTK; NKPTSLWNPTyGSWFTEKPTKK	1	2	2	2
1586	HFPCGNVNYGyQQQGLPLEAATAPGAGHYEDtILK				1

pY, phospho-tyrosine. "y" in the peptide sequence represents phospho-tyrosine.

Figure 1. Identification of aberrantly phosphorylated RTKs in 60 ovarian cancer patients. A, elevated tyrosine phosphorylation (phosphotyrosine) of RTKs in 60 ovarian tumors. Hierarchical clustering of elevated tyrosine phosphorylation in 26 RTKs across 60 ovarian tumors using MultiExperiment Viewer Version 4.4 (MeV). Elevated phosphotyrosine level of 0.2 or higher are shown with indicated colors. Gray spots represent data points with no phosphotyrosine level increase or no assigned phosphotyrosine spectrum. B, ranking of RTK tyrosine phosphorylation in ovarian cancer. RTKs are ranked based on the average value of elevated phosphotyrosine count in tumors with increased phosphotyrosine of each RTK. Data were visualized using MeV with the same color scale as in A. The number of tumors with elevated phosphotyrosine level of each RTK is shown in parentheses. C, ALK phosphotyrosine sites identified by LC/MS–MS mass spectrometry in 4 ovarian tumor patients. Peptide sequences and spectral counts of juxtamembrane sites (Y1078 1092, and 1096), kinase domain sites (Y1278, 1282, and 1283), and carboxyl terminal sites (Y1507, 1586) are shown.

discoidin domain receptors (DDR), ephrin receptor kinases (EphA, EphB), as well as EGFR and FGFR family kinases. Interestingly, ALK was ranked as the top kinase with the highest elevated tyrosine phosphorylation among other RTKs (Fig. 1B).

ALK phosphorylation was found in 4 patients, including 3 serous carcinoma patients OC07, OC16, and OC26 and a stromal sarcoma patient OC19 (Fig. 1C). Hyperphosphorylation of ALK in OC19 is indicated by multiple phosphotyrosine sites in the juxtamembrane, kinase, and C-terminal regulatory domains, many of which were seen previously in other type of cancers (data not shown). Phosphorylation of Y1507, which is equivalent to Y567 in NPM-ALK found in anaplastic large cell lymphoma, was detected in all 4 patients (Fig. 1C). This phospho site was also observed in primary tumor tissues and cell lines of NSCLC bearing EML-ALK fusions, as well as neuroblastoma cell lines bearing ALK-activating mutations (data not shown). Extracted ion chromatograms, MS2 spectra of 2 tryptic peptides containing phosho-Y1507 indicated the detection of ALK peptides in these patients (Supplementary Fig. S1A and B).

Previous studies have shown that Y1507 (Y527 in NPM-ALK) located at the carboxyl terminal region of ALK is a direct docking site for SH2 domain-containing transforming protein (SHC1). Recruitment and phosphorylation of SHC1 activate Ras/extracellular signal–regulated kinase (ERK) pathway and promotes tumorigenesis (27, 28). Consistent with these observations, using label-free quantification analysis, we found hyperphosphorylation of SHC1, mitogen-activated protein kinase 14 (MAPK14), and CDK1 at specific sites (Supplementary Fig. S2 and Table S3) in the 3 serous carcinoma patients bearing ALK phosphorylation. In addition, phosphorylation of other ALK downstream signaling molecules, including those that are involved in Jak/Stat3, PI3K/AKT pathways, are upregulated in these tumors (Supplementary Fig. S2 and Table S3). These results suggested that in serous carcinoma patients OC07, OC16, and OC26, ALK might contribute to activation of multiple

Published OnlineFirst May 8, 2012; DOI: 10.1158/0008-5472.CAN-11-3931

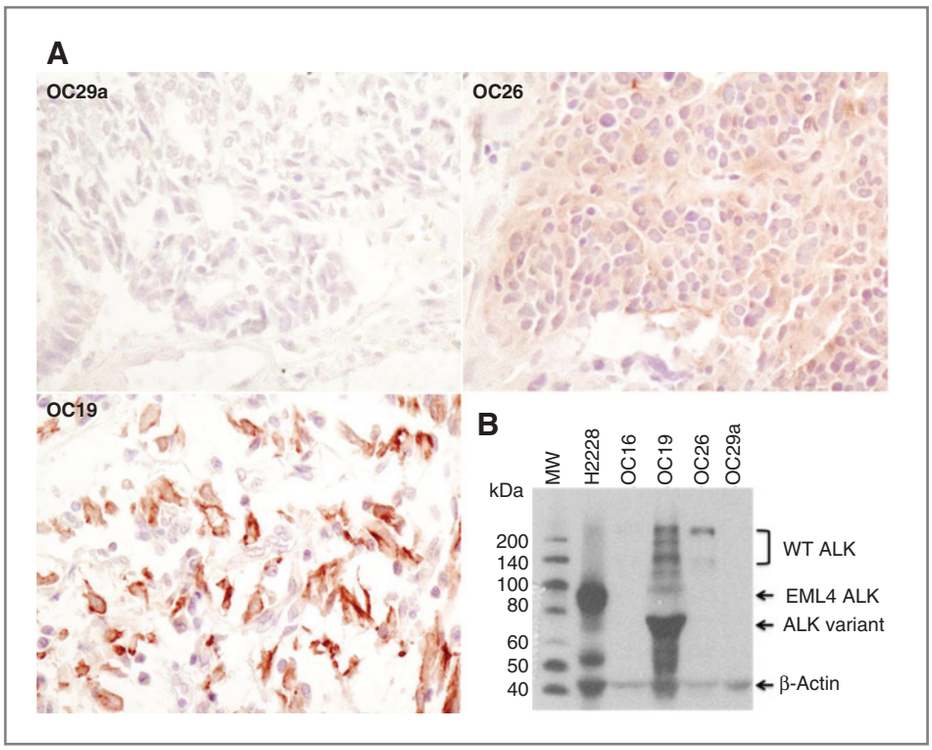

Figure 2. ALK protein expression in ovarian cancer patients. A, immunohistochemical staining of paraffin sections of ovarian tissue from serous carcinoma patients OC29a, OC26, and stromal sarcoma patient OC19 with an antibody against ALK kinase domain. Images represent ×40 magnification. B, Western blot analysis of protein lysates from serous carcinoma tissue OC16, OC26, and OC29a or stromal sarcoma patient OC19, as well as a lung cancer cell line H2228 carrying EML4-ALK fusion using antibodies against ALK and β-actin as a loading control. Positions of wild-type (WT) ALK (both full length and the 140 kDa cleaved forms), EML4-ALK and approximately 78 kDa ALK variant are indicated.

signaling pathways that promote tumor cell survival, growth, and proliferation.

Taken together, we found 4 of 69 (5.8%) ovarian cancer patients carrying phosphorylated ALK at sites that correlate with ALK oncogenesis, including 3 of 43 (7.0%) serous carcinoma and one stromal sarcoma patients. To our knowledge, this is the first time that ALK tyrosine phosphorylation is described in ovarian cancer.

Using an antibody directed against the ALK intracellular domain, we examined ALK protein localization and expression by immunohistochemical and Western blot analysis with patient tissue (Fig. 2). Similar to neuroblastoma cells and tumor tissues that overexpress ALK (21), we observed a diffused ALK staining at the cytoplasm of serous carcinoma OC26, but not in other serous carcinoma tissues such as OC29a (Fig. 2A). In the stromal tumor OC19, strong ALK signal is present at both the plasma membrane and the cytoplasm, with membrane accentuation in some cells (Fig. 2A). Western blot analysis detected mature full-length ALK at 220 kDa in OC16 and OC26, and the potential proteolytically cleaved 140 kDa form (29) in OC26, which might be too weak to be detected in OC16. We identified multiple ALK signals of variable sizes in OC19, with the most prominent signal at approximately 78 kDa, suggesting the presence of a novel form of ALK different from the EML4-ALK Variant 3 fusion protein in the lung cancer cell line H2228 (Fig. 2B). These results suggested that OC19 might carry a different gene translocation involving ALK.

As a neuronal receptor kinase, ALK is not normally expressed in the ovary. Expression and phosphorylation of ALK in 4 ovarian cancer patients prompted us to test whether the *ALK* gene in these patients may have undergone genetic alterations. As the activating mutations previously reported in neuroblastoma (18–20) were not detected in the cytoplasmic region of ALK in OC07, OC16, OC26, and OC19 (data not shown), we set out to examine other possible genetic alterations of ALK.

ALK gene copy number gain in serous carcinoma tissues

In neuroblastoma, *ALK* was identified as a recurrent target of copy number gain and gene amplification (18, 19, 21). Recent study conducted by The Cancer Genome Atlas (TCGA) research network indicated a remarkable degree of genomic disarray in serous carcinoma (30). To examine whether there is copy number variation (CNV) of *ALK* in ovarian tumors in which ALK phosphorylation was detected, we used real-time quantitative PCR with genomic DNA isolated from serous carcinoma OC07, OC16, OC26, and stromal sarcoma OC19, as well as serous carcinoma OC08, in which ALK phosphorylation is not detected. Although no obvious CNV of *ALK* was detected in OC08 and OC19, ALK copy number gains of 1.5- and 1.7-fold were detected in OC16 and OC26, respectively (Fig. 3A). The result is consistent with our high-resolution single-nucleotide polymorphism array analysis, which indicated a copy number of 3 in the *ALK* region in patient OC26 (data not shown). The *ALK* copy number gain in OC16 and OC26 may account for the aberrant expression of ALK in these serous carcinoma patients. Surprisingly, we observed a loss of *ALK* gene copies in serous carcinoma OC07 (Fig. 3A), in which ALK phosphorylation (Fig. 1A and C, Supplementary Fig. S1) and mRNA expression (see below) were detected, suggesting

Published OnlineFirst May 8, 2012; DOI: 10.1158/0008-5472.CAN-11-3931

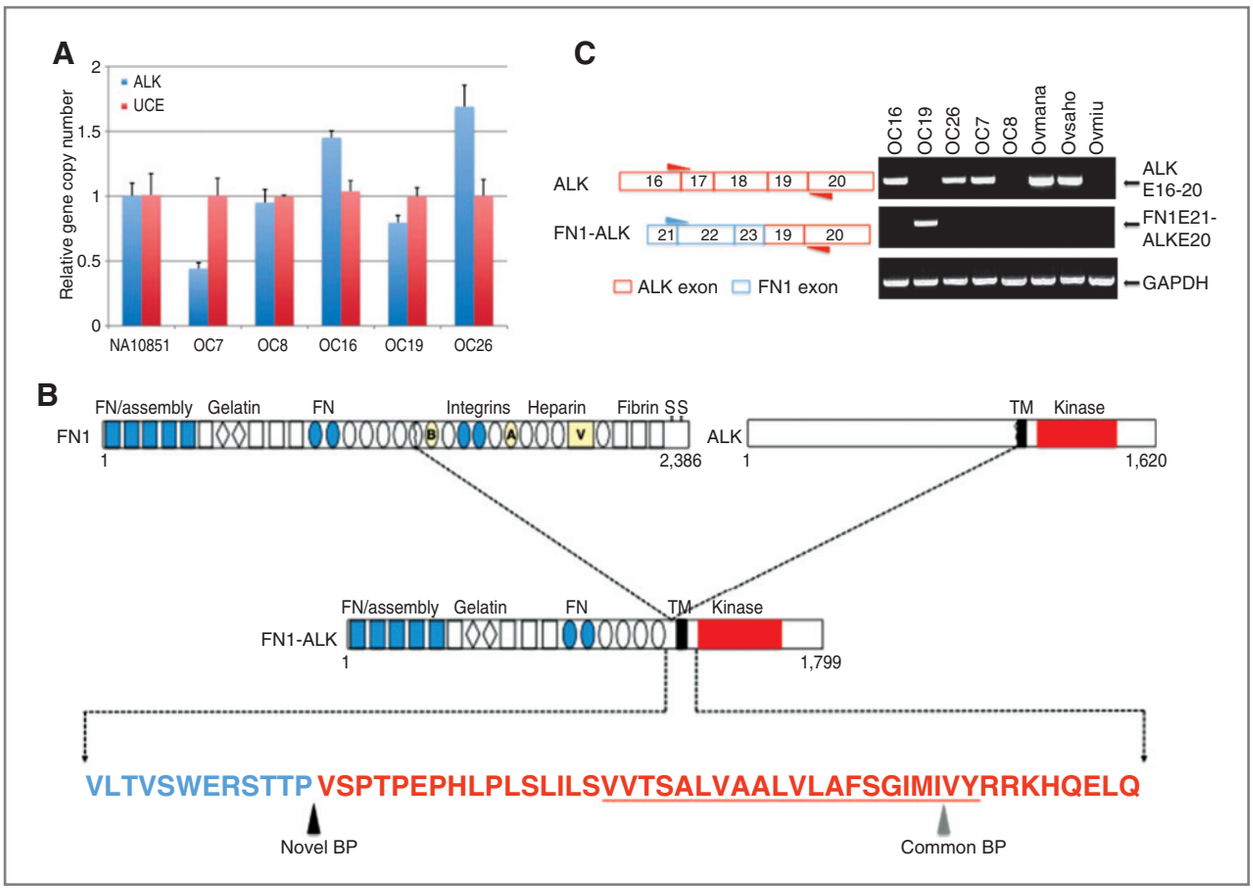

Figure 3. Genetic characterization of ovarian tumors with ALK phosphorylation. A, ALK gene CNV in serous carcinoma patients. qPCR analysis was carried out with genomic DNA isolated from tumor tissue OC07, OC08, OC16, OC19, and OC26. The value of relative gene copy number of ALK to that of UCE in each gDNA sample is shown. Calculations were carried out to normalize a copy number of 2 to a value of 1 in the bar graph. SDs were based on duplicate normalized C_t values. This result represents 3 independent experiments. B, identification of a novel fusion protein, FN1-ALK, in a stromal sarcoma patient, OC19. Fusion of the aminoterminal 1,201 amino acids of FN1 to the carboxyl terminal 598 amino acids containing the transmembrane (TM) and the intracellular kinase domain of ALK. The types I, II, and III modules in FN1 are shown in rectangles, diamonds, and ovals, respectively, with domains required for fibrillogenesis shaded in blue. Domains subjected to alternative splicing in various fibronectin isoforms are shaded in light yellow (B, A, and V). The positions of FN1 domains involved in binding to various ECM proteins are indicated. The ALK amino acid positions of the novel breakpoint (Novel BP, black arrow) in FN1-ALK and the common breakpoint (Common BP, gray arrow) are indicated. C, RT-PCR analysis of full-length ALK or FN1-ALK expression in ovarian tumor tissue and cell lines. The positions of PCR primers used to amplify the ALK cDNA region from exon 16 to exon 20 and the FN1-ALK cDNA region from FN1 exon 21 to ALK exon 20 are indicated. Exons in ALK and FN1 are indicated in red and blue, respectively. Amplification of GAPDH is used as a qualitative control of the cDNA samples.

that aberrant ALK expression and phosphorylation is independent of *ALK* copy number in this patient.

Identification of a novel fusion protein FN1-ALK in a malignant stromal sarcoma patient

Fusion of ALK kinase domain to a partner protein, resulting in constitutive activation of ALK and oncogenesis in non-Hodgkin lymphoma (17), NSCLC (15, 22, 31), inflammatory myofibroblastic tumor (23), and renal cell carcinoma (24, 25) has been reported previously. Given the presence of highly phosphorylated ALK with differing sizes in patient OC19 and the fact that no *ALK* mutation or copy number gain was detected in this patient, we suspected the presence of an *ALK* gene translocation. To test this possibility, we carried out 5′-RACE with RNA isolated from OC19 tumor. Because the majority of previously reported *ALK* fusions have a common breakpoint between exons 19 and 20 (15, 17, 22–25, 31), we searched the sequences upstream of this common breakpoint using a primer annealing to the 5′ end of exon 20. Cloning and sequence determination of the RACE product revealed that *ALK* is fused in frame to *fibronectin 1* (*FN1*), encoding a ubiquitous component of extracellular matrix (ECM) and plasma (32), at a novel breakpoint between *ALK* exons 18 and 19. The resultant fusion protein FN1-ALK contains the amino-terminal 1,201 amino acids of FN1 and the carboxyl-terminal 598 amino acids of ALK, which include the transmembrane and cytoplasmic regions (Fig. 3B). Encoded by the first 23 exons, the FN1 portion of FN1-ALK retains a diverse set of binding domains involved in fibronectin self-association and interaction with other ECM components,

Published OnlineFirst May 8, 2012; DOI: 10.1158/0008-5472.CAN-11-3931

which could potentially provide strong activating signal to ALK (Fig. 3B). Unlike previous ALK fusions, the novel breakpoint in FN1-ALK allows the ALK transmembrane region to be retained in the fusion protein (Fig. 3B). The predicted protein sequence of full-length FN1-ALK is shown in Supplementary Fig. S3B.

To test mRNA expression of FN1-ALK or full-length ALK in tumors with ALK phosphorylation, we carried out RT-PCR analysis with primers that specifically amplify fragments from FN1-ALK or full-length ALK cDNA (Fig. 3C). ALK mRNA expression was observed in the 3 serous carcinoma patients, OC07, OC16, and OC26, as well as in 2 ovarian cell lines, OVMANA and OVSAHO (Fig. 3C). In contrast, only FN1-ALK mRNA, but not full-length ALK mRNA, was detected in OC19 (Fig. 3C). As expected, neither full-length ALK nor FN1-ALK mRNA was detected in OC08 and the ovarian cancer cell line Ovmiu. These results indicated that FN1-ALK fusion is present in the stromal sarcoma patient OC19, whereas full-length ALK expression resides in serous carcinoma patients OC07, OC16, and OC26.

To examine the *FN1-ALK* gene fusion at genomic level, we used PCR primers annealing to the 3′ end of *FN1* exon 23 and the 5′ end of *ALK* exon 19 to amplify DNA sequence spanning the joint of these 2 genes. Sequences of the PCR product revealed that the first 946 base pairs of *FN1* intron 23 were fused to the last 14 base pairs of *ALK* intron 18 (Supplementary Fig. S3A). Given that *ALK* and *FN1* map to the short and long arm of chromosome 2 (2p23 and 2q34), respectively, in the same orientation, it remains to be determined whether the formation of the *FN1-ALK* fusion was caused by a large interstitial deletion spanning the centromere or other chromosomal changes.

Transforming potential of ALK and FN1-ALK

To determine whether full-length ALK and FN1-ALK have transforming potential, we generated NIH3T3 cells stably expressing full-length ALK or FN1-ALK (Fig. 4A and B). As expected, we observed both full-length ALK (220 kDa) and the 140 kDa cleaved ALK (29, 33) in 3T3/ALK cells. Interestingly, in addition to full-length FN1-ALK proteins (predicted

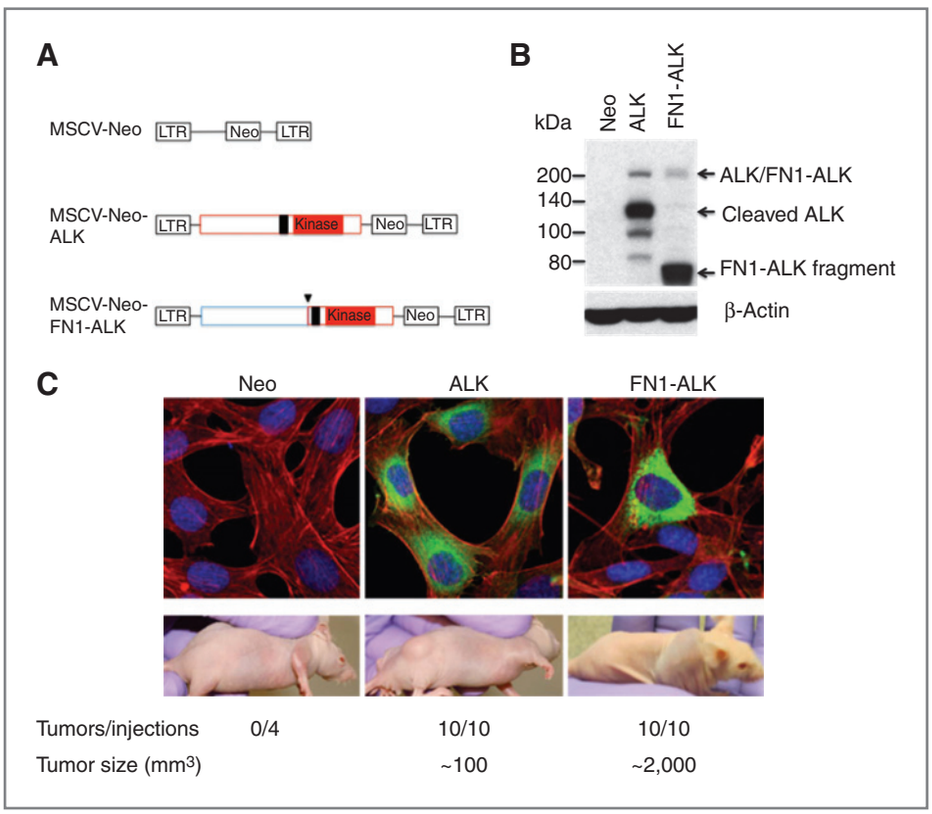

Figure 4. Oncogenic potential of ALK and FN1-ALK. A, schematic diagram of MSCV constructs used to generate stably transfected NIH 3T3 cells. ALK and FN1 cDNA sequences are indicated with red or blue boxes, respectively. ALK kinase domain and transmembrane domain are shaded in red and black, respectively. Note the joint of FN1 and ALK, which is indicated with an arrow. Neo, neomycin; LTR, long terminal repeat. B, Western blot analysis of protein lysates prepared from 3T3 cells stably transfected with Neo, ALK, or FN1-ALK. Positions of the full-length ALK or FN1-ALK, 140 kDa cleaved ALK in 3T3/ALK cells and approximately 78 kDa FN1-ALK fragment in 3T3/FN1-ALK cells, respectively. Western blot with anti-β-actin antibody was used as loading control. C, immunofluorescence analysis of stably transfected 3T3 cells and *in vivo* tumorigenicity assay. Immunofluorescent analysis was done with stably transfected 3T3 cells expressing neomycin (Neo), ALK, or FN1-ALK using D5F3 XP antibody against ALK (green), DY-554 phalloidin for actin filaments (red), and DRAQ5 for DNA (blue). 3T3 cells expressing Neo, ALK, or FN1-ALK are injected subcutaneously into nude mice. The tumor images, the rate of tumor growth, and the average size of tumors are reported 12 days after injection. The results are representative of 2 independent experiments.

Published OnlineFirst May 8, 2012; DOI: 10.1158/0008-5472.CAN-11-3931

molecular weight: 198.82 kDa), which migrates at approximately 225 kDa, we observed a prominent ALK signal of approximately 78 kDa in 3T3/FN1-ALK cells, which is a reminiscence of the strong ALK signal in patient OC19 tumor (Fig. 4B, Fig. 2B). We suspected that this approximately 78 kDa protein is a fragment derived from full-length FN1-ALK. Both ALK and FN1-ALK showed intracellular reticulum/Golgi localization (Fig. 4C), as indicated by immunofluorescence analysis, probably due to a defect of glycosylation of these overexpressed proteins in 3T3 cells (33). When 3T3/Neo, 3T3/ALK, or 3T3/FN1-ALK cells were injected subcutaneously into nude mice, we observed tumor growth induced by both 3T3/ALK and 3T3/FN1-ALK cells, with the FN1-ALK tumors growing more aggressively than the ALK tumors (Fig. 4C). The average tumor sizes 12 days after injection were around 2,000 mm^3 and 100 mm^3 for FN1-ALK and ALK tumors, respectively. If allowed to grow, ALK tumors could reach approximately 2,000 mm^3 20 days after injection (data not shown). These results indicated that both the full-length ALK and the FN1-ALK fusion isolated from the ovarian cancer patients have transforming potential and that FN1-ALK is more oncogenic than the full-length ALK.

To investigate downstream signaling pathways activated by full-length ALK and FN1-ALK, we analyzed endogenous signaling molecules of 293T cells when they overexpress full-length ALK and FN1-ALK. Both full-length ALK and FN1-ALK showed constitutive activation as indicated by the phosphorylation of tyrosine sites in their kinase domain (Supplementary Fig. S4). Interestingly, the 140 kDa cleaved ALK and the approximately 78 kDa FN1-ALK fragment had stronger phosphorylation than their full-length forms. Consistent with ALK activation, phosphorylation of Stat3, SHC, and Erk was upregulated, with FN1-ALK cells showing stronger upregulation of these molecules than ALK cells (Supplementary Fig. S4). ALK inhibitor crizotinib abolished phosphorylation of both ALK and FN1-ALK. As expected, phosphorylation of Stat3, SHC, and Erk was also diminished upon crizotinib treatment (Supplementary Fig. S4). Another ALK inhibitor TAE684 showed similar results (data not shown). These results indicated that, similar to what we observed in patient tumors using phosphoproteomic approach, expression of both ALK and FN1-ALK in 293T cells leads to activation of multiple downstream signaling molecules, which can be inhibited by ALK inhibitors. In addition, the stronger oncogenic activity of FN1-ALK than full-length ALK might be attributed to its stronger potential in activating downstream molecules, such as Stat3, SHC, and Erk, whose activation contributes to cell growth and proliferation.

ALK and FN1-ALK as potential therapeutic target

Both PF-02341066 (crizotinib) and TAE684 are potent and selective ALK inhibitors that have been shown to suppress tumor cell growth in several types of cancers expressing different ALK fusion proteins (34–38). We tested the effects of these inhibitors on the growth of ALK and FN1-ALK tumors in nude mice. As shown in Fig. 5A, administration of crizotinib (100 mg/kg/d) drastically inhibited the growth of both ALK and FN1-ALK tumors, but not the 3T3/SRC tumors. Consistent with these observations, Western blot analysis using antibodies specific for ALK and phospho-ALK revealed that crizotinib abolished phosphorylation of both full-length FN1-ALK and the approximately 78 kDa ALK variant 24 hours after treatment (Fig. 5B). We also observed an ALK signal with lower molecular weight next to the full-length FN1-ALK in crizotinib-treated tumor, which is likely to be a signal of nonphophorylated FN1-ALK (Fig. 5B). Similar tumor growth-inhibiting effects were observed with TAE684 (Supplementary Fig. S5). These results suggested that ALK and FN1-ALK tumors are highly sensitive to ALK inhibitors.

Detection of ALK expression in a larger patient cohort

To test possible aberrant ALK expression in a larger patient cohort, we carried out immunohistochemical analysis on ovarian TMAs. Similar to what we observed in the Chinese cohort (69 tumors) using PhosphoScan, although no ALK staining was detected in normal tissues, granulosa-theca cell tumors, or clear cell carcinomas, ALK staining was detected in 14 of 353 (4%) serous carcinoma and 3 of 37 endometrioid carcinoma specimens, with half of the specimens having strong ALK signal (Fig. 6A and B). We observed mostly weak ALK staining in some mucinous carcinoma specimens (Fig. 6A, images not shown). Consistent with what we found in patient OC26, most of the ALK staining observed in serous carcinomas in TMA was diffusedly localized in the cytoplasm (Fig. 6B). This result suggested that ALK might be activated and signaling in these tumors, similar to what has been observed in neuroblastomas, in which full-length ALK is overexpressed (21). Considering that a significant number of high-grade serous carcinoma has been misclassified as endometrioid carcinoma (1, 39), our data suggested that strong ALK expression resides mainly in a portion (~2%) of serous carcinoma.

Discussion

Oncogenic role of ALK has been well characterized in many types of hematopoietic and solid tumors, in which ALK is deregulated by gene translocations, activating mutations, and amplification (15, 17–25, 31, 40, 41). Although ALK transcript was reported to be present in epithelial ovarian cancer (42), ALK protein expression and phosphorylation in ovarian cancer has not been reported. Using a phosphoproteomic approach, we identified ALK tyrosine phosphorylation in 4 of 69 primary ovarian tumor tissues. Further investigation revealed *ALK* gene copy number gain in 2 serous carcinoma patients and a novel *ALK* gene translocation (*FN1-ALK*) in a stromal sarcoma patient. Mouse 3T3 fibroblasts overexpressing full-length ALK or FN1-ALK generated subcutaneous tumor in nude mice. In addition, we showed that ALK inhibitors dramatically suppressed the growth of both 3T3 ALK and 3T3 FN1-ALK tumors. This study provides new insight into the molecular pathogenesis of ovarian cancer and compelling rationale for extending targeted therapy against ALK to this new type of solid tumor.

Oncogenic role of full-length ALK has been implicated in neuroblastoma (21), glioblastoma (43), and breast cancer (44).

Published OnlineFirst May 8, 2012; DOI: 10.1158/0008-5472.CAN-11-3931

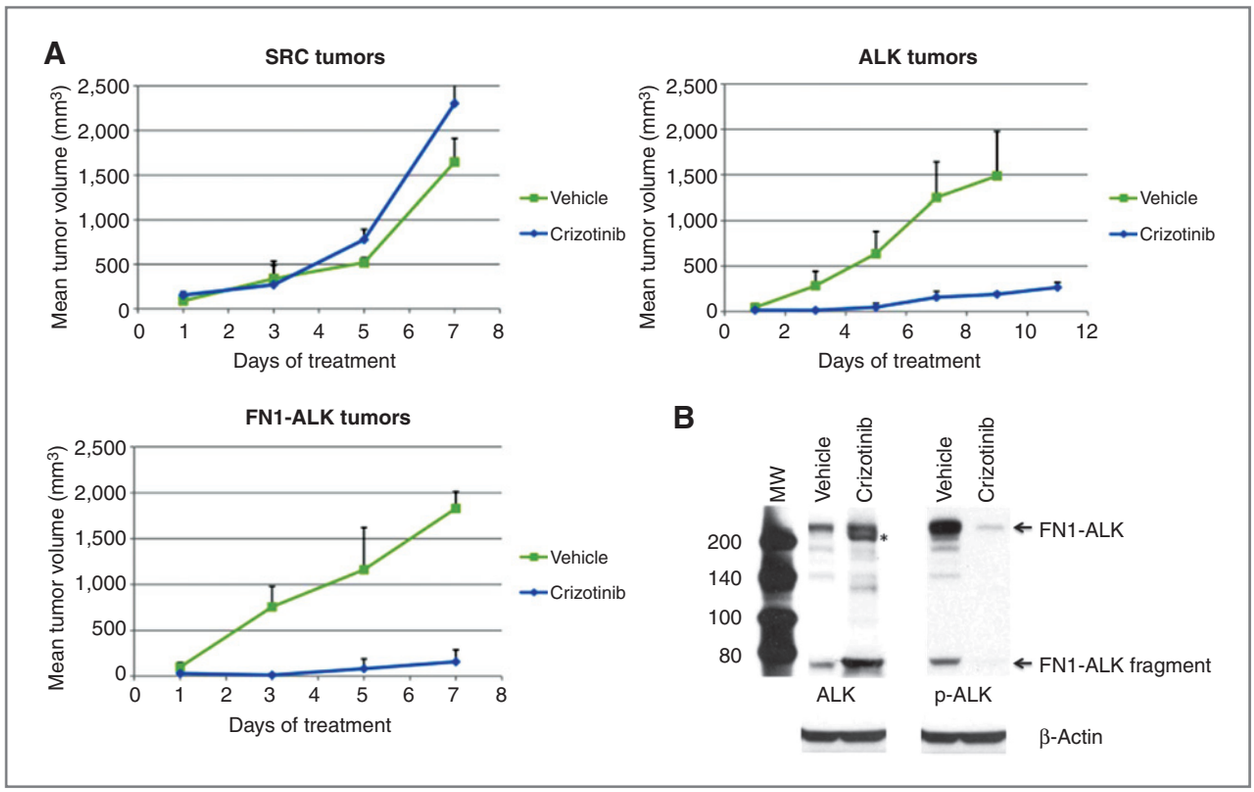

Figure 5. ALK and FN1-ALK tumors are sensitive to an ALK inhibitor, crizotinib. A, four to 6 nude mice carrying 3T3 tumors expressing Src, ALK, or FN1-ALK are treated with vehicle or 100 mg/kg/d crizotinib by oral gavage when tumors are palpable (~50 mm^3). The tumors are measured every other day until the mean tumor size of the vehicle treated mice reaches 1,500 mm^3. B, mice carrying FN1-ALK tumors were treated with vehicle or crizotinib for 24 hours before the tumors were harvested and analyzed by Western blot assay using antibodies against ALK, phospho-ALK (Y1278/1282/1283), and β-actin. Arrows indicate the positions of the full-length FN1-ALK and the approximately 78 kDa truncated ALK variant. Note an ALK signal with lower molecular weight (*) next to the FN1-ALK, which is likely nonphosphorylated FN1-ALK.

Consistent with a recent report from TCGA Research Network, in which 489 high-grade serous ovarian adenocarcinomas were analyzed (30), we did not find any activating mutation or significant gene amplification of ALK in 41 serous carcinoma patients. However, our data showed phosphorylation of full-length ALK at Y1507 in 3 serous carcinoma patients, 2 of which have *ALK* gene copy number gain. The phosphorylation of multiple downstream signaling molecules such as SHC1, STAT3, tyrosine kinases (SYK, FRK, and FYN), SHIP 2 (INPPL1), MAPK14, CDK1, and phosphoinositide 3-kinase (PI3K), are upregulated compared with other serous carcinoma patients. These results indicate that previously reported Ras/ERK, Jak3/Stat3, and PI3K/Akt pathways, which mediate the effect of ALK activity and promote tumor cell proliferation and survival (27, 28), are activated in ALK-bearing serous carcinoma patients. Our proteomic approach also identified many other molecules such as NEDD9 and PKCδ (PRKCD) that are involved in transformation (45, 46) in these patients, although their relevance to ALK activity has yet to be determined. Aberrant expression, phosphorylation, cytoplasmic localization, as well as activation of ALK downstream signaling pathways suggest an oncogenic role of full-length ALK in serous ovarian carcinoma. Interestingly, unlike 3T3/FN1-ALK cells, 3T3/ALK cells did not generate transformed colonies in soft agar assay (data not shown). However, they generated tumors in nude mice. We suspect that full-length ALK could be activated through paracrine signaling under *in vivo* conditions. Functional validation using more pathologically relevant models such as primary tumor xenografts or fallopian tube secretory epithelial cell (4) models will be helpful in assessing the transforming effects of ALK and determine how full-length ALK is activated in serous carcinomas.

The novel fusion protein FN1-ALK identified in a stromal sarcoma patient represents the first ALK fusion protein bearing the transmembrane domain of ALK itself. Fusion to the *FN1* gene that encodes a ubiquitously expressed ECM protein likely causes high-level expression of the ALK kinase. Unlike most ALK fusion partner proteins that render ALK constitutive activity through homodimerization, FN1 may do so through its strong interactions with ECM structures and components such as fibrin, heparin, collagen, and gelatin. Because fibronectin is subjected to proteolytic breakdown by a number of neutral proteases (47), the approximately 78 kDa fragment of FN1-ALK that we observed in both the patient tumor and transfected 3T3 or 293T cells is likely a proteolytically cleaved product of full-length FN1-ALK (~220 kDa). Strong expression, hyperphosphorylation, and membrane/cytoplasmic localizations of ALK suggest

Published OnlineFirst May 8, 2012; DOI: 10.1158/0008-5472.CAN-11-3931

A

Ovarian tissue type	Total	ALK + (%)	ALK ++/ +++ (%)
Serous carcinoma	353	7 (2.0%)	7 (2.0%)
Endometrioid carcinoma	37	2 (5.4%)	1 (2.2%)
Mucinous carcinoma	88	7 (8.0%)	0
Clear cell carcinoma	14	0	0
Granulosa-theca cell tumor	19	0	0
Normal	37	0	0

B

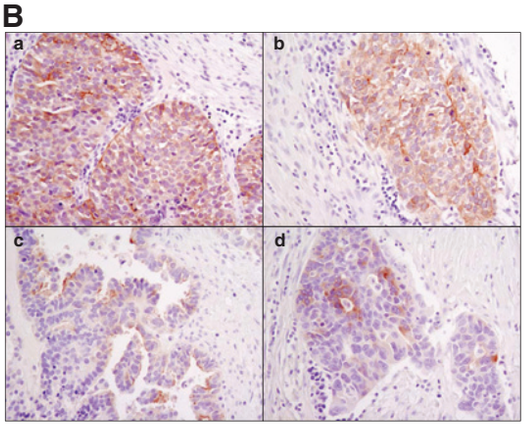

Figure 6. Aberrant ALK expression in a larger patient cohort detected by immunohistochemical analysis of ovarian TMA. A, immunohistochemical analysis of FFPE ovarian TMAs were carried out ALK (D5F3) XP rabbit mAb as described in Materials and Methods. Total specimen numbers of each subtype and numbers of ALK weak (+) or strong (++ or +++) specimens are listed. B, images from 4 serous carcinoma specimen that are ALK+++ (a and b) and ALK++ (c and d), representing ×40 magnification.

constitutive internalization and activation of FN1-ALK, which may lead to its strong oncogenic potential, as evidenced by the strong activation of downstream molecules in 293T cells and the *in vivo* tumorigenecity assay. Considering the sensitivity of 3T3/FN1-ALK tumors to ALK inhibitors and the recent promising results of treating inflammatory myofibroblastic tumor (IMT) with ALK inhibitor crizotinib (38), we expect optimistic response of stromal sarcoma patients carrying FN1-ALK to targeted therapy against ALK. Our discovery broadens the scope of ALK fusion oncoproteins in human cancer and identifies a compelling therapeutic target in a new type of mesenchymal neoplasm.

To overcome chemoresistance and to improve the overall survival of ovarian cancer patients, targeted therapy has come to the forefront of investigation. Among reported oncogenes (8) associated with ovarian cancer identified to date, EGFR received substantial attention as a therapeutic target because of its overexpression in 70% ovarian cancer patients (48). However, inhibitors and monoclonal antibodies against EGFR only resulted in marginal efficacy due to toxic side effects and lack of inhibitor-sensitizing *EGFR* mutations in ovarian cancer patients (49). Unlike EGFR, which is ubiquitously expressed in normal tissue, ALK expression is restricted to certain parts of the brain (50). This might explain why inhibition of ALK has little toxic effects in patients (28). As shown recently in NSCLC and IMT patients, ALK inhibitor crizotinib only showed grade 2 side effects at a dose of 250 mg twice daily (37, 38). Compared with 10% response rate to second-line chemotherapy, the response rate of NSCLC patients carrying the EML4-ALK fusion to crizotinib is 57% (37). Given the presence of an ALK-driven subgroup of ovarian cancer, especially serous carcinoma patients, and the fact that crizotinib inhibited ALK or FN1-ALK tumor growth and activation of downstream signaling molecules, we speculate that crizotinib or other ALK-targeting agent may become effective treatment in these patients.

Besides ALK inhibitors, other therapeutic options for ALK bearing ovarian cancer patients might also be considered. First, coexpression/activation of other RTKs in ALK-bearing serous carcinoma patients, such as Ret (in OC26) (21), suggests that combinational therapy against multiple RTK could provide better outcome. Second, as ALK expression is tumor specific in ovarian cancer, antibody-mediated immunotherapy against ALK could be highly efficient with little damage to normal tissue. Third, as previously shown in anaplastic large cell lymphoma (28), ALK is likely to be highly immunogenic in ovarian cancer patients and thus could be an ideal target for antitumor vaccination in these patients.

Combining our results from the Chinese patient cohort and the immunohistochemical analysis of TMA containing more than 400 ovarian tumors of a distinct patient cohort, we estimate that 2% to 4% high-grade serous ovarian carcinoma patients have aberrant ALK expression. Given the annual approximately 140,000 worldwide new cases and approximately 7,000 deaths from high-grade serous ovarian carcinoma, the number of patients who might benefit from targeted therapy against ALK could be substantial.

Disclosure of Potential Conflicts of Interest

No potential conflicts of interest were disclosed.

Acknowledgments

The authors thank Michael Lewis, Roy Scialdone, Curtis Desilets, Joan MacMeill, Julie Nardone, Cindy Reeves, and Yi Wang for technical support and Yu Li, Roberto Polakiewicz, and Long Ma for critical comments.

Grant Support

This study was partially supported by a grant from National Natural Science Foundation of China, 81101475, to Z.-P. Tan, X. Zhu, and Y.-F. Yang.

The costs of publication of this article were defrayed in part by the payment of page charges. This article must therefore be hereby marked *advertisement* in accordance with 18 U.S.C. Section 1734 solely to indicate this fact.

Received December 2, 2011; revised February 27, 2012; accepted April 26, 2012; published OnlineFirst May 8, 2012.

References

1. Vaughan S, Coward JI, Bast RC Jr., Berchuck A, Berek JS, Brenton JD, et al. Rethinking ovarian cancer: recommendations for improving outcomes. Nat Rev Cancer 2011;11:719–25.

2. Kurman RJ, Shih IM. The origin and pathogenesis of epithelial ovarian cancer: a proposed unifying theory. Am J Surg Pathol 2010; 34:433–43.

Published OnlineFirst May 8, 2012; DOI: 10.1158/0008-5472.CAN-11-3931

3. Bell DA. Origins and molecular pathology of ovarian cancer. Mod Pathol 2005;18 Suppl 2:S19–32.
4. Karst AM, Levanon K, Drapkin R. Modeling high-grade serous ovarian carcinogenesis from the fallopian tube. Proc Natl Acad Sci U S A 2011;108:7547–52.
5. Levanon K, Crum C, Drapkin R. New insights into the pathogenesis of serous ovarian cancer and its clinical impact. J Clin Oncol 2008;26: 5284–93.
6. Willmott LJ, Fruehauf JP. Targeted therapy in ovarian cancer. J Oncol 2010:740472.
7. Modesitt SC, Jazaeri AA. Recurrent epithelial ovarian cancer: pharmacotherapy and novel therapeutics. Expert Opin Pharmacother 2007;8:2293–305.
8. Bast RC Jr., Hennessy B, Mills GB. The biology of ovarian cancer: new opportunities for translation. Nat Rev Cancer 2009;9:415–28.
9. Sheng Q, Liu X, Fleming E, Yuan K, Piao H, Chen J, et al. An activated ErbB3/NRG1 autocrine loop supports *in vivo* proliferation in ovarian cancer cells. Cancer Cell 2010;17:298–310.
10. Apte SM, Bucana CD, Killion JJ, Gershenson DM, Fidler IJ. Expression of platelet-derived growth factor and activated receptor in clinical specimens of epithelial ovarian cancer and ovarian carcinoma cell lines. Gynecol Oncol 2004;93:78–86.
11. Psyrri A, Kassar M, Yu Z, Bamias A, Weinberger PM, Markakis S, et al. Effect of epidermal growth factor receptor expression level on survival in patients with epithelial ovarian cancer. Clin Cancer Res 2005; 11:8637–43.
12. Shepard HM, Lewis GD, Sarup JC, Fendly BM, Maneval D, Mordenti J, et al. Monoclonal antibody therapy of human cancer: taking the HER2 protooncogene to the clinic. J Clin Immunol 1991;11:117–27.
13. Tanner B, Hasenclever D, Stern K, Schormann W, Bezler M, Hermes M, et al. ErbB-3 predicts survival in ovarian cancer. J Clin Oncol 2006;24: 4317–23.
14. Rush J, Moritz A, Lee KA, Guo A, Goss VL, Spek EJ, et al. Immunoaffinity profiling of tyrosine phosphorylation in cancer cells. Nat Biotechnol 2005;23:94–101.
15. Rikova K, Guo A, Zeng Q, Possemato A, Yu J, Haack H, et al. Global survey of phosphotyrosine signaling identifies oncogenic kinases in lung cancer. Cell 2007;131:1190–203.
16. Gu TL, Deng X, Huang F, Tucker M, Crosby K, Rimkunas V, et al. Survey of tyrosine kinase signaling reveals ROS kinase fusions in human cholangiocarcinoma. PLoS One 2011;6:e15640.
17. Morris SW, Kirstein MN, Valentine MB, Dittmer KG, Shapiro DN, Saltman DL, et al. Fusion of a kinase gene, ALK, to a nucleolar protein gene, NPM, in non-Hodgkin's lymphoma. Science 1994; 263:1281–4.
18. Janoueix-Lerosey I, Lequin D, Brugieres L, Ribeiro A, de Pontual L, Combaret V, et al. Somatic and germline activating mutations of the ALK kinase receptor in neuroblastoma. Nature 2008;455:967–70.
19. Chen Y, Takita J, Choi YL, Kato M, Ohira M, Sanada M, et al. Oncogenic mutations of ALK kinase in neuroblastoma. Nature 2008; 455:971–4.
20. George RE, Sanda T, Hanna M, Frohling S, Luther W 2nd, Zhang J, et al. Activating mutations in ALK provide a therapeutic target in neuroblastoma. Nature 2008;455:975–8.
21. Osajima-Hakomori Y, Miyake I, Ohira M, Nakagawara A, Nakagawa A, Sakai R. Biological role of anaplastic lymphoma kinase in neuroblastoma. Am J Pathol 2005;167:213–22.
22. Soda M, Choi YL, Enomoto M, Takada S, Yamashita Y, Ishikawa S, et al. Identification of the transforming EML4-ALK fusion gene in non-small-cell lung cancer. Nature 2007;448:561–6.
23. Lawrence B, Perez-Atayde A, Hibbard MK, Rubin BP, Dal Cin P, Pinkus JL, et al. TPM3-ALK and TPM4-ALK oncogenes in inflammatory myofibroblastic tumors. Am J Pathol 2000;157:377–84.
24. Debelenko LV, Raimondi SC, Daw N, Shivakumar BR, Huang D, Nelson M, et al. Renal cell carcinoma with novel VCL-ALK fusion: new representative of ALK-associated tumor spectrum. Mod Pathol 2010;24: 430–42.
25. Marino-Enriquez A, Ou WB, Weldon CB, Fletcher JA, Perez-Atayde AR. ALK rearrangement in sickle cell trait-associated renal medullary carcinoma. Genes Chromosomes Cancer 2010;50:146–53.
26. Deutsch EW, Mendoza L, Shteynberg D, Farrah T, Lam H, Tasman N, et al. A guided tour of the Trans-Proteomic Pipeline. Proteomics 2010;10:1150–9.
27. Fujimoto J, Shiota M, Iwahara T, Seki N, Satoh H, Mori S, et al. Characterization of the transforming activity of p80, a hyperphosphorylated protein in a Ki-1 lymphoma cell line with chromosomal translocation t(2;5). Proc Natl Acad Sci U S A 1996;93:4181–6.
28. Chiarle R, Voena C, Ambrogio C, Piva R, Inghirami G. The anaplastic lymphoma kinase in the pathogenesis of cancer. Nat Rev Cancer 2008;8:11–23.
29. Moog-Lutz C, Degoutin J, Gouzi JY, Frobert Y, Brunet-de Carvalho N, Bureau J, et al. Activation and inhibition of anaplastic lymphoma kinase receptor tyrosine kinase by monoclonal antibodies and absence of agonist activity of pleiotrophin. J Biol Chem 2005;280:26039–48.
30. Network TCGAR. Integrated genomic analyses of ovarian carcinoma. Nature 2011;474:609–15.
31. Takeuchi K, Choi YL, Togashi Y, Soda M, Hatano S, Inamura K, et al. KIF5B-ALK, a novel fusion oncokinase identified by an immunohistochemistry-based diagnostic system for ALK-positive lung cancer. Clin Cancer Res 2009;15:3143–9.
32. Schwarzbauer JE, DeSimone DW. Fibronectins, their fibrillogenesis, and *in vivo* functions. Cold Spring Harb Perspect Biol 2011;3: a005041.
33. Mazot P, Cazes A, Boutterin MC, Figueiredo A, Raynal V, Combaret V, et al. The constitutive activity of the ALK mutated at positions F1174 or R1275 impairs receptor trafficking. Oncogene 2011;30:2017–25.
34. Christensen JG, Zou HY, Arango ME, Li Q, Lee JH, McDonnell SR, et al. Cytoreductive antitumor activity of PF-2341066, a novel inhibitor of anaplastic lymphoma kinase and c-Met, in experimental models of anaplastic large-cell lymphoma. Mol Cancer Ther 2007;6:3314–22.
35. Galkin AV, Melnick JS, Kim S, Hood TL, Li N, Li L, et al. Identification of NVP-TAE684, a potent, selective, and efficacious inhibitor of NPM-ALK. Proc Natl Acad Sci U S A 2007;104:270–5.
36. Zou HY, Li Q, Lee JH, Arango ME, McDonnell SR, Yamazaki S, et al. An orally available small-molecule inhibitor of c-Met, PF-2341066, exhibits cytoreductive antitumor efficacy through antiproliferative and antiangiogenic mechanisms. Cancer Res 2007;67:4408–17.
37. Kwak EL, Bang YJ, Camidge DR, Shaw AT, Solomon B, Maki RG, et al. Anaplastic lymphoma kinase inhibition in non-small-cell lung cancer. N Engl J Med 2010;363:1693–703.
38. Butrynski JE, D'Adamo DR, Hornick JL, Dal Cin P, Antonescu CR, Jhanwar SC, et al. Crizotinib in ALK-rearranged inflammatory myofibroblastic tumor. N Engl J Med 2010;363:1727–33.
39. Kelemen LE, Kobel M. Mucinous carcinomas of the ovary and colorectum: different organ, same dilemma. Lancet Oncol 2011;12: 1071–80.
40. Mosse YP, Laudenslager M, Longo L, Cole KA, Wood A, Attiyeh EF, et al. Identification of ALK as a major familial neuroblastoma predisposition gene. Nature 2008;455:930–5.
41. Griffin CA, Hawkins AL, Dvorak C, Henkle C, Ellingham T, Perlman EJ. Recurrent involvement of 2p23 in inflammatory myofibroblastic tumors. Cancer Res 1999;59:2776–80.
42. Pejovic T, Pande NT, Mori M, Mhawech-Fauceglia P, Harrington C, Mongoue-Tchokote S, et al. Expression profiling of the ovarian surface kinome reveals candidate genes for early neoplastic changes. Transl Oncol 2009;2:341–9.
43. Powers C, Aigner A, Stoica GE, McDonnell K, Wellstein A. Pleiotrophin signaling through anaplastic lymphoma kinase is rate-limiting for glioblastoma growth. J Biol Chem 2002;277:14153–8.
44. Perez-Pinera P, Chang Y, Astudillo A, Mortimer J, Deuel TF. Anaplastic lymphoma kinase is expressed in different subtypes of human breast cancer. Biochem Biophys Res Commun 2007;358: 399–403.
45. Izumchenko E, Singh MK, Plotnikova OV, Tikhmyanova N, Little JL, Serebriiskii IG, et al. NEDD9 promotes oncogenic signaling in mammary tumor development. Cancer Res 2009;69: 7198–206.
46. Grossoni VC, Falbo KB, Kazanietz MG, de Kier Joffe ED, Urtreger AJ. Protein kinase C delta enhances proliferation and survival of murine mammary cells. Mol Carcinog 2007;46:381–90.

Published OnlineFirst May 8, 2012; DOI: 10.1158/0008-5472.CAN-11-3931

47. Labat-Robert J. Fibronectin in malignancy. Semin Cancer Biol 2002; 12:187–95.
48. Yap TA, Carden CP, Kaye SB. Beyond chemotherapy: targeted therapies in ovarian cancer. Nat Rev Cancer 2009;9:167–81.
49. Mustea A, Sehouli J, Fabjani G, Koensgen D, Mobus V, Braicu EI, et al. Epidermal growth factor receptor (EGFR) mutation does not correlate with platinum resistance in ovarian carcinoma. Results of a prospective pilot study. Anticancer Res 2007;27:1527–30.
50. Webb TR, Slavish J, George RE, Look AT, Xue L, Jiang Q, et al. Anaplastic lymphoma kinase: role in cancer pathogenesis and small-molecule inhibitor development for therapy. Expert Rev Anticancer Ther 2009;9:331–56.

Published OnlineFirst May 8, 2012; DOI: 10.1158/0008-5472.CAN-11-3931

Cancer Research
The Journal of Cancer Research (1916–1930) | The American Journal of Cancer (1931–1940)

AACR American Association for Cancer Research

Identification of Anaplastic Lymphoma Kinase as a Potential Therapeutic Target in Ovarian Cancer

Hong Ren, Zhi-Ping Tan, Xin Zhu, et al.

Cancer Res 2012;72:3312-3323. Published OnlineFirst May 8, 2012.